



# A New Stochastic Model to Improve Positioning Accuracy of the Recursive Least Squares Method

Nerjes Rahemi\*, Kurosh Zarrinigar\* and Mohammad Reza Mosavi\*(C.A.)

**Abstract:** In determining position using GPS, due to local effects, pseudo-range errors cannot be mitigated by methods such as the use of reference stations or mathematical models; however, by using precise carrier phase observations and deploying a statistically optimal filter such as Phase-Adjusted Pseudo-range (PAPR) algorithm, the error can be significantly reduced. Additionally, the correlation between observations is a factor affecting positioning accuracy. In this paper, by using both pseudo-range and carrier phase observations and taking into account the effect of spatial correlation between observations to determine the variance-covariance matrix, the accuracy of position determination using the recursive Least Squares method is increased. For this purpose, the PAPR algorithm was implemented to reduce error. Next, a non-diagonal variance-covariance matrix was introduced to estimate the variance of the observations based on their spatial correlations. Experimental results on real data show that the proposed method improves positioning accuracy by at least 10% compared to previous methods. To evaluate the complexity of the proposed models, we employed an ARM STM32H743 processor. The findings indicate a modest increase in the proposed model complexity compared to earlier models, along with a substantial improvement in positioning accuracy.

**Keywords:** GPS, Phase-Adjusted Pseudo-range Algorithm, Recursive Least Squares, Spatial Correlations, Variance-Covariance Matrix.

## 1 Introduction

THE final stage of a GPS software receiver involves solving navigation equations and determining the position. In this stage, the navigation equations are formed using pseudo-range and carrier phase observations from at least four satellites. Then, by solving these equations, the position is determined.

There are two primary methods for solving navigation equations: (1) The Least Squares (LS) algorithm and (2) the Kalman Filter (KF). In the LS algorithm, the position is obtained by minimizing the sum of the residual

squares of each equation. In contrast, the KF is an optimal estimator that employs the state-space concept and the system error models to provide an optimal estimate of the system state using a series of noisy measurements [1,2].

To accurately describe the motion of a target, the KF requires a dynamic model to obtain prior knowledge about how the target moves. Its performance significantly depends on the quality of this model. Choosing an inappropriate model, especially when GPS observations are distorted due to phenomena such as signal loss, multi-path effects, and so on, can lead to reduced filter performance or even divergence. On the other hand, compared to the LS, KF is used in positioning in a smaller dynamic range of the user, i.e., the conditions in which the acceleration derivative does not exceed  $2g$  (where  $g$  represents gravitational acceleration). When the user is in high dynamic conditions, adopting KF position and velocity results leads to reduced performance. This is due to inaccuracies in the estimation of the highest order state

*Iranian Journal of Electrical & Electronic Engineering*, 2025.

Paper first received 19 Nov. 2024 and accepted 04 Mar. 2025.

\* The authors are with the School of Electrical Engineering, Iran University of Science and Technology (IUST), Narmak, Tehran 16846-13114, Iran.

E-mails: [Rahemi@iust.ac.ir](mailto:Rahemi@iust.ac.ir), [k\\_zarrinigar@elec.iust.ac.ir](mailto:k_zarrinigar@elec.iust.ac.ir), and [m\\_mosavi@iust.ac.ir](mailto:m_mosavi@iust.ac.ir)

Corresponding Author: Mohammad Reza Mosavi

estimations, which causes the model to mismatch at the moments of high acceleration derivatives [3].

To achieve higher accuracy in real-time positioning using single-frequency GPS receivers, various methods have been proposed, such as: differential positioning, integration with other navigation systems, use of supplementary tools, etc. However, these methods generally entail significant complexity and high implementation costs [4-6].

In determining the GPS receiver's position, pseudo-range observations play a central role. The main sources of error include ionospheric and tropospheric errors, satellite clock and orbit errors, and the pseudo-range errors. The first two errors can be corrected by methods such as using augmentation corrections from reference stations or using the mathematical models; however, since pseudo-range errors are local effects, they cannot be corrected by these methods. In this situation, carrier phase observations can significantly reduce the error.

Two common methods for reducing pseudo-range noise using carrier phase measurements are the Hatch smoothing algorithm and the phase-connected pseudo-range algorithm [7-9]. In the Hatch algorithm, a recursive process is used to calculate the receiver location, epoch after epoch; however, the severe time correlations between pseudo-range observations in differential applications prevent the model from functioning recursively. In this algorithm, these correlations are ignored. In the phase-connected pseudo-range algorithm, differential carrier phase observations from two consecutive epochs are used along with code observations. In this algorithm, the correlation is lower than in the Hatch algorithm but still cannot be ignored, making it impossible to estimate the position using a recursive method. Therefore, these algorithms are not optimal solutions [10,11].

Another proposed algorithm for this purpose is the Phase-Adjusted Pseudo-range (PAPR) algorithm, which is more efficient than previous methods [10,12]. In this algorithm, a Recursive Least Squares (RLS) filter is applied with code and carrier phase observations used simultaneously in a unified model, where the carrier phase ambiguities are considered unknown constant parameters. These unknown parameters, along with the positioning parameters, are recursively estimated [11,13]. This method minimizes the computational load and preserves all information. It has been proven to be statistically optimal and fully models the system's behavior.

To accurately determine the position, a stochastic model is needed to estimate the statistical characteristics of the observations [14-16]. Existing models generally use either the elevation angle or SNR of the observations [17,18]. By assuming insignificant spatial correlations

between observations, they obtain the variance-covariance matrix in a diagonal form while considering spatial correlations between non-differential observations, which can lead to higher accuracy.

In this paper, positioning using the PAPR algorithm is performed with non-differential data in a single-frequency GPS receiver and its performance is compared with the Least Squares method. Next, to increase the accuracy, two non-diagonal variance-covariance matrices were introduced to estimate the variance of the observations their spatial correlations.

The proposed method is implemented on a receiver and tested with real-time data. Experiments show that the proposed method improved positioning accuracy by at least 40% compared to the LS method and by at least 10% compared to diagonal VCM-based methods.

This paper is organized as follows. In the second section, the PAPR algorithm is described. The third section presents the proposed method for estimating the variance of observations. The fourth section presents the experimental results and their analysis. Finally, the conclusion is presented in the last section of the paper.

## 2 Positioning using Phase-Adjusted Pseudo-range Algorithm

The PAPR algorithm is an optimal solution in which all observations (code and carrier phase measurements) are used in a unified model, with ambiguities and position parameters estimated by an RLS solution [19]. In this method, observations are used non-differentially. The following presents the equations for this method.

The observation equations are as follows:

$$E\left\{\begin{pmatrix} \underline{P}_1 \\ \underline{\Phi}_1 \\ \underline{P}_2 \\ \underline{\Phi}_2 \\ \vdots \\ \underline{P}_k \\ \underline{\Phi}_k \end{pmatrix}\right\} = \begin{pmatrix} A_1 & & 0 \\ A_1 & & I \\ & A_2 & 0 \\ & A_2 & I \\ & & \ddots \\ & & \vdots \\ & & A_k & 0 \\ & & A_k & I \end{pmatrix} \begin{pmatrix} x_1 \\ x_2 \\ \vdots \\ x_k \\ \nabla \end{pmatrix} \quad (1)$$

$$D\left\{\begin{pmatrix} \underline{P}_1 \\ \underline{\Phi}_1 \\ \underline{P}_2 \\ \underline{\Phi}_2 \\ \vdots \\ \underline{P}_k \\ \underline{\Phi}_k \end{pmatrix}\right\} = \begin{pmatrix} Q_{P_1} & & & & 0 \\ & Q_{\phi_1} & & & \\ & & Q_{P_2} & & \\ & & & Q_{\phi_2} & \\ & & & & \ddots \\ & & & & & Q_{P_k} \\ 0 & & & & & & Q_{\phi_k} \end{pmatrix} \quad (2)$$

where  $\underline{P}_i$  is the linearized pseudo-range vector at epoch  $t_i$ ,  $\underline{x}_i$  is the vector of unknown parameters at epoch  $t_i$ ,  $\underline{\Phi}_i$  is the vector of linearized carrier phases at epoch  $t_i$ ,  $A_i$  is the linearized design matrix at epoch  $t_i$ ,  $\nabla$  is the vector of unknown ambiguities, and  $\mathcal{Q}_{\underline{P}_i}$  and  $\mathcal{Q}_{\underline{\Phi}_i}$  are the variance matrix of code and carrier phase measurements at epoch  $t_i$ , respectively. Thus, the recursive equations for the position parameters can be expressed as follows:

$$\hat{\underline{x}}_k = \mathcal{Q}_{\hat{\underline{x}}_k} A_k^T (\mathcal{Q}_{\underline{P}_k}^{-1} \underline{P}_k + [\mathcal{Q}_{\Phi_k} + \mathcal{Q}_{\hat{\nabla}_{k-1}}]^{-1} [\underline{\Phi}_k - \hat{\nabla}_{k-1}]) \quad (3)$$

$$\mathcal{Q}_{\hat{\underline{x}}_k} = [A_k^T (\mathcal{Q}_{\underline{P}_k}^{-1} + [\mathcal{Q}_{\Phi_k} + \mathcal{Q}_{\hat{\nabla}_{k-1}}]^{-1}) A_k]^{-1} \quad (4)$$

Additionally, the updated values of ambiguities can be obtained using Equations (5) and (6):

$$\hat{\nabla}_k = \hat{\nabla}_{k-1} + \mathcal{Q}_{\hat{\nabla}_{k-1}} [\mathcal{Q}_{\underline{P}_k} + \mathcal{Q}_{\hat{\nabla}_{k-1}}]^{-1} [\underline{\Phi}_k - \hat{\nabla}_{k-1} - A_k \hat{\underline{x}}_k] \quad (5)$$

$$\begin{aligned} \mathcal{Q}_{\hat{\nabla}_k} &= \mathcal{Q}_{\hat{\nabla}_{k-1}} - \mathcal{Q}_{\hat{\nabla}_{k-1}} [\mathcal{Q}_{\Phi_k} + \mathcal{Q}_{\hat{\nabla}_{k-1}}]^{-1} \mathcal{Q}_{\hat{\nabla}_{k-1}} + \\ &\mathcal{Q}_{\hat{\nabla}_{k-1}} [\mathcal{Q}_{\Phi_k} + \mathcal{Q}_{\hat{\nabla}_{k-1}}]^{-1} A_k \mathcal{Q}_{\hat{\underline{x}}_k} A_k^T [\mathcal{Q}_{\Phi_k} + \mathcal{Q}_{\hat{\nabla}_{k-1}}]^{-1} \mathcal{Q}_{\hat{\nabla}_{k-1}} \end{aligned} \quad (6)$$

The initial values of the parameters  $\hat{\underline{x}}_1$ ,  $\hat{\nabla}_1$ ,  $\mathcal{Q}_{\hat{\underline{x}}_1}$ , and  $\mathcal{Q}_{\hat{\nabla}_1}$  are obtained from a Least Square solution [20].

This algorithm is optimal as it completely models the behavior of the system and requires no additional assumptions, except the assumption that there is no time correlation between epochs.

To estimate the position based on the PAPR algorithm, the following steps must be performed:

1. Formation of linearized pseudo-range and carrier phases vectors  $\underline{P}_0$ ,  $\underline{\Phi}_0$  and the design matrix  $A_0$  with the initial values of the observations.

It should be noted that the linearized matrices are obtained from the difference between the observed pseudo-range and the calculated pseudo-range based on the current position of the satellite and the user.

2. Estimation of the initial epoch's position parameters and ambiguities and their variance matrices from the LS solution.

3. Formation of the linearized pseudo-range and carrier phases vectors and the design matrix at epoch  $t_i$  ( $\underline{P}_i$ ,  $\underline{\Phi}_i$  and  $A_i$ ) based on the observations at that epoch.

4. Updating the position parameters at epoch  $t_i$  using Equations (3) and (4).

5. Updating the values of ambiguities at epoch  $t_i$  using Equations (5) and (6).

6. Repetition of steps 3 to 5 until the observations continue.

As mentioned earlier, in standalone positioning, the main sources of error are satellite clocks and orbits, tropospheric and ionospheric delays and the pseudo-range noise. Except for code noise, other sources can be compensated using products, such as global ionosphere maps, precise ephemerides, and a precise tropospheric model. However, the code noise, which is significantly large in this positioning mode, cannot be mitigated in the same way. Therefore, this positioning mode greatly benefits from filtering with carrier phase observations to reduce pseudo-range noise.

### 3 Variance Estimation Method

Appropriate weighting of observations is essential because GPS measurements taken at different epochs or from different satellites do not have the same accuracy. In other words, the quality of observations differs. This variation is mainly due to factors such as random noise, correlation between observations, tracking loop characteristics, receiver dynamics, signal strength, multipath, atmospheric effects, etc. Therefore, assigning a higher weight to accurate observations, which contribute more to parameter estimation than imprecise ones, reduces the impact of low-quality observations. As a result, positioning accuracy is improved [19].

The weighting method used in the VCM ensures that observations are included in the RLS algorithm based on their reliability. This approach improves the accuracy of the solution by prioritizing high-quality data while reducing the impact of less accurate or highly correlated observations. The VCM, defined based on the stochastic model, represents the statistical characteristics of GPS observations. The main diagonal elements (variances) represent observation accuracy, while the non-diagonal elements (covariances) represent the correlations between observations [21,22].

A complete variance-covariance matrix is defined in Equation (7):

$$\mathbf{R}_k = \begin{bmatrix} \sigma_{1,1}^2 & \sigma_{1,2} & \cdots & \sigma_{1,n} \\ \sigma_{2,1} & \sigma_{2,2}^2 & & \sigma_{2,n} \\ \vdots & & \ddots & \vdots \\ \sigma_{n,1} & \sigma_{2,n} & \cdots & \sigma_{n,n}^2 \end{bmatrix} \quad (7)$$

where  $\sigma_{i,i}^2$  represents the measurement noise variance of the  $i$ -th observation (variances) and  $\sigma_{i,j}$  represents the measurement noise variance between the  $i$ -th and  $j$ -th observation (covariances).

The VCM can be defined in two ways: diagonal and non-diagonal. Using a diagonal matrix, where physical correlations between GPS measurements are neglected,

leads to less accurate positioning results. The use of a simplified VCM, containing only diagonal variance elements, leads to biased parameter estimates and overly optimistic formal accuracy measures. Correlations between observations make the non-diagonal elements of the VCM non-zero. A suitable stochastic model for GPS observations should account for both the observation quality indicators and the possible correlation of GPS observations [23].

Physical correlations include three types: spatial, temporal, and cross-correlations, representing correlations in space, over time, and between frequencies, respectively. Temporal correlation, which refers to correlations between observations at different epochs, is significant in GPS differential observations for relative positioning. In non-differential conditions, its value can be neglected because the differentiation process increases the time correlation of phase observations. The cross-correlation is also significant between L1 and L2 carriers but negligible between phase and code observations. Finally, spatial correlation refers to the correlation between observations from different satellites at the same time and location due to similar observational conditions [23].

Based on the above explanations and considering that non-differential pseudo-range observations are used for positioning in this paper, spatial correlation is considered, while other correlations with negligible values are ignored. In addition, as the trigonometric model is one of the most common and accurate models for variance estimation, it is used here to complete the stochastic model for both code and phase measurements. In the proposed VCM for  $n$  satellites, taking into account the spatial correlation between the observations, the variances and covariances are defined according to Equations (8) and (9), respectively:

$$\sigma_{i,i}^2 = \frac{1}{\sin^2(El_i)} \quad \text{or} \quad \sigma_{i,i}^2 = \frac{1}{\tan^2(El_i - \theta_0)} \quad (8)$$

$$\sigma_{i,j}^2 = \frac{\alpha}{\sin(El_i)\sin(El_j)} \quad \text{or} \quad (9)$$

$$\sigma_{i,j}^2 = \frac{\alpha}{\tan(El_i - \theta_0)\tan(El_j - \theta_0)}$$

where  $El_i$  indicates the elevation angle of the  $i$ -th satellite,  $\theta_0$  is a reference elevation angle, and  $\alpha$  is a weighting factor to model the covariance between different satellites.

Figure 1 shows the variance curves obtained from the sinusoidal and tangential models with respect to the elevation angle. Also, Fig. 2 illustrates the variances and covariances of two satellites at different elevation angles using the proposed VCM based on the sinusoidal model.

## 4 Experimental Results

This section presents and analyzes the experimental results of the proposed method. In all experiments, a single-frequency PPP approach was implemented. The proposed methods are applied to raw data or GPS observations from a U-Blox ZED-F9T receiver. The experiments have been statically at a location within the Iran University of Science and Technology. The test setup and the test location are shown in Figs. 3 and 4, respectively.

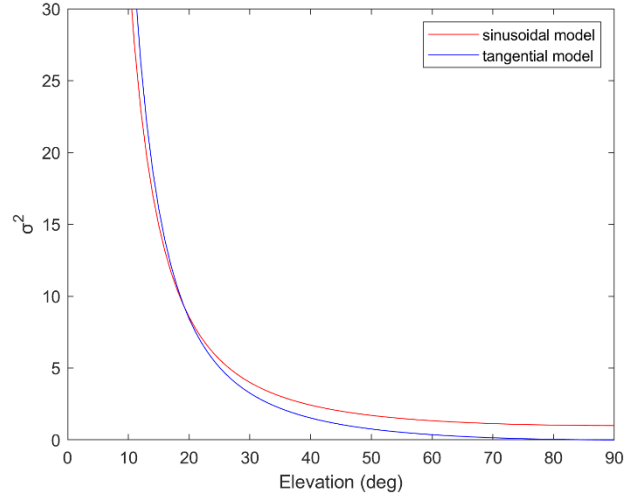


**Fig 1.** The variance curves based on the sinusoidal and tangential models.

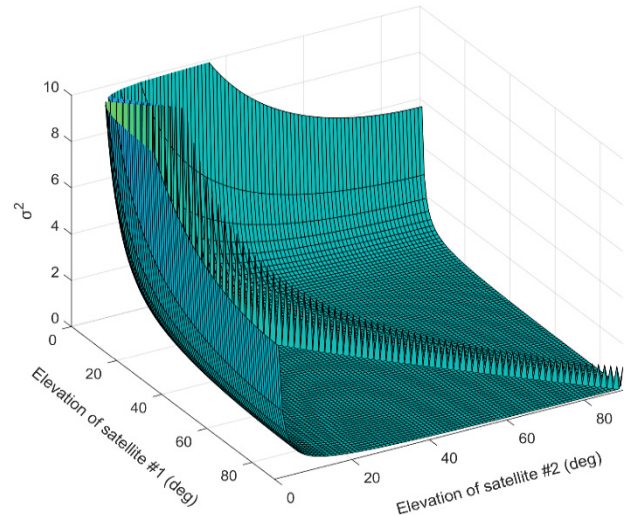


**Fig 2.** The variances and covariances of two satellites for different elevation angles using the proposed VCM based on the sinusoidal model.

The flowchart used for positioning is presented in Fig. 5. To evaluate the performance of the proposed method, positioning was performed using the LS method, the KF and the PAPR algorithm, along with four different observation weighting methods (diagonal VCM based on sinusoidal and tangential models, and the proposed

VCM based on sinusoidal and tangential models). Figure 6 shows the positioning error of the aforementioned methods, and the RMS values of the positioning errors obtained from the different methods are presented in Table 1.

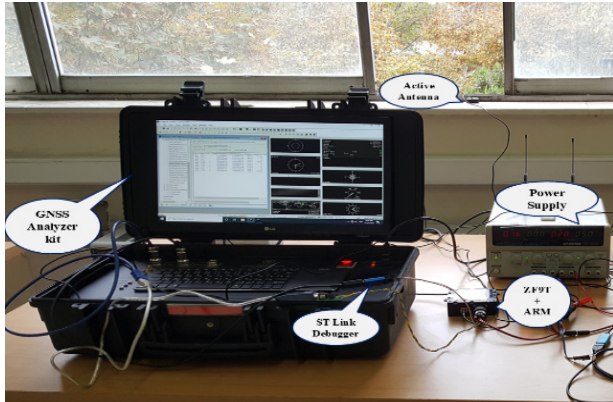


Fig 3. The test setup.



Fig 4. The location of the tests.

The LS method shows the highest error, and the use of the PAPR algorithm reduces this error. Additionally, the proposed VCM shows better results than the diagonal VCM, and among the two proposed VCMs, the tangential model provides more accurate positioning. Error fluctuations in this method are smaller than in the other methods. Finally, among all the methods, the PAPR algorithm combined with the proposed VCM based on the tangential model achieves the best positioning accuracy.

In the next step, to further evaluate the efficiency of the methods, Cumulative Distribution Function (CDF) and Probability Density Function (PDF) curves of the errors were generated. These curves are shown in Figs. 7 and 8, respectively, and the statistical parameters derived from these curves are provided in Table 2.

As shown in Fig. 7, the CDF curve of the PAPR algorithm combined with the proposed VCM based on the tangential model exhibits lower error values compared to other methods. As seen in Fig. 8, the peak

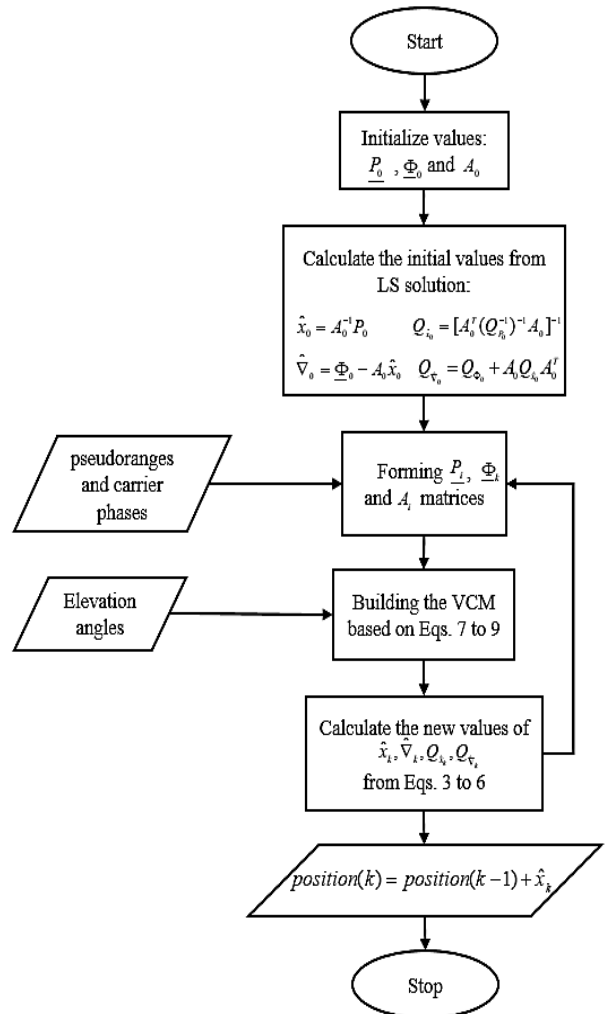


Fig 5. The flowchart of positioning.

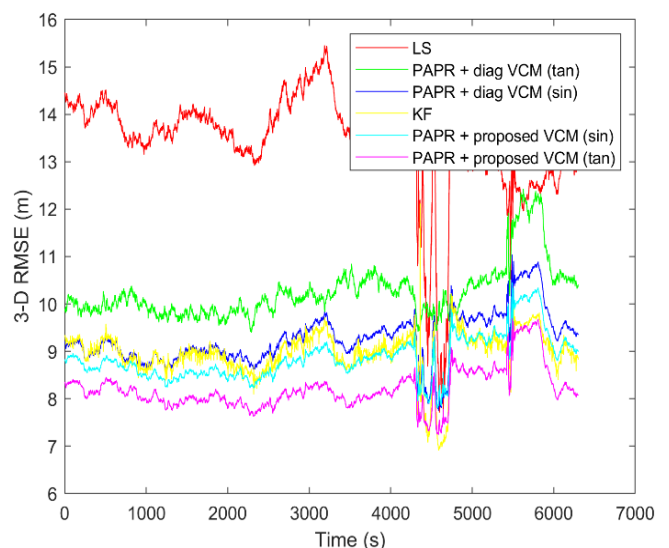


Fig 6. The positioning error of different methods.

of the PDF curve for the mentioned method occurs at lower error values, and the curve's width is smaller than that of the other methods, indicating the superior performance of this method.

**Table 1.** The positioning error of different methods in meters.

Method	RMSE
LS	13.48
PAPR + diag VCM (tan)	10.26
PAPR + diag VCM (sin)	9.28
KF	8.97
PAPR + proposed VCM (sin)	8.87
PAPR + proposed VCM (tan)	8.22

**Table 2.** The positioning error of different methods in meters.

Method	Average Error	STD of Error	Error (0%95)
LS	13.43	1.1	15.25
PAPR + diag VCM (tan)	10.25	0.56	11.19
PAPR + diag VCM (sin)	9.26	0.53	10.15
KF	8.96	0.47	9.74
PAPR + proposed VCM (sin)	8.85	0.46	9.63
PAPR + proposed VCM (tan)	8.21	0.43	8.91

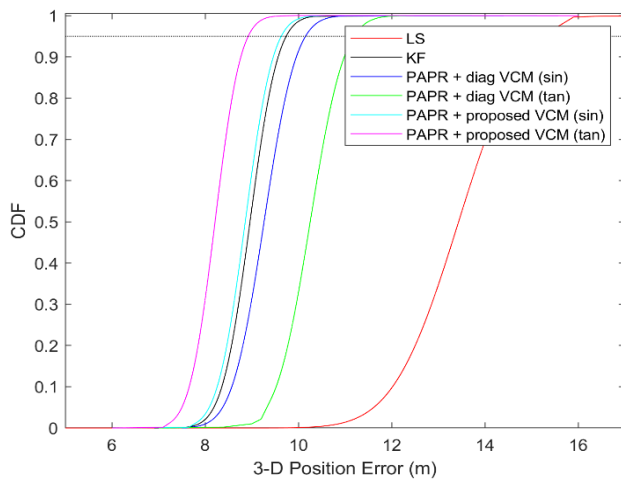


**Fig 7.** The CDF of different methods.

Table 2 shows that the PAPR algorithm, combined with the proposed VCM based on the tangential model, performs better than other methods in terms of mean error, standard deviation of error, and 95% error.

Therefore, based on the obtained results, it can be concluded that the PAPR, combined with the proposed tangential-based VCM, provides better stability, smoothness, and accuracy than other methods.

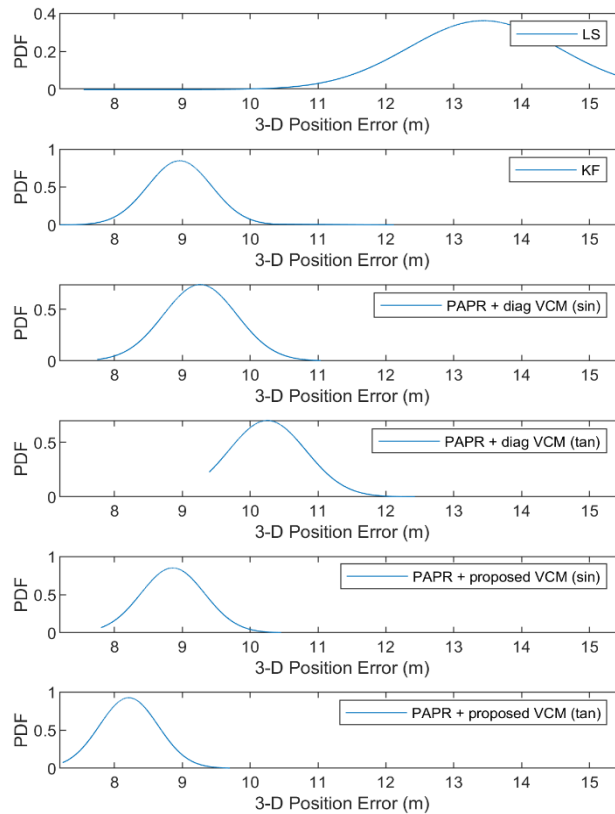


**Fig 8.** The PDF of different methods.

In further analyzing the proposed methods, it is important to note that in the practical application, assigning realistic weights to observations presents a challenge. Variance models that rely on elevation angles typically assume a direct relationship between the satellite's elevation and the quality of the GPS signal. However, these models are inadequate for measurements heavily impacted by signal diffraction patterns or receiver characteristics. Consequently, when dealing with measurements acquired under less-than-ideal conditions, considering direct signal quality measures, such as Signal-to-Noise Ratio (SNR), can further improve performance.

Given that the presented methods deal with matrix calculations, the dimensions of the matrix depend on the number of satellites the receiver uses in navigation. On the other hand, some observations, such as the pseudo-range, are from the order of  $1e6$ . Therefore, quantum errors in expressing numbers, such as rounding decimal numbers, or errors caused by hardware, such as overflow and number of bits limitation in FPU computations, cause the positioning calculation to deviate from the actual value. Besides that, memory plays a significant role in keeping observations for each proposed method. The more satellites in the receiver's field of view, the more memory is needed to store GPS observations temporarily. As a result, hardware implementation is limited regarding processor speed and memory.

The STM32H743 microcontroller is a powerful processor for complicated matrix calculations. According to Fig. 3 and 4, the complexity of the proposed models based on GPS observations was evaluated using an STM32H743 32-bit Cortex-M7 ARM processor, operating at a maximum frequency of 480 MHz, alongside a Ublox ZED-F9T receiver. The processor features an IEEE 754-compliant FPU, enabling high-precision decimal calculations. GPS observations were collected in stationary mode at a 10 Hz update rate with the Ublox ZED-F9T receiver. Table 3 provides a comparative analysis of the complexity of the implemented methods.

**Table 3.** Comparison of hardware implementation complexity of different methods.

Method	PT [ $\mu$ Sec]	Flash Memory Usage [kByte]	Total Memory Usage (%)
LS	4.8	14.54	0.71
PAPR + diag VCM (tan)	2.2	22.25	1.08
PAPR + diag VCM (sin)	1.3	21.61	1.05
KF	1.3	20.51	1
PAPR + proposed VCM (sin)	1.4	21.99	1.07
PAPR + proposed VCM (tan)	2.3	22.64	1.1

Table 3 indicates that the Least Squares error method has a high Processing Time (PT) per sample, primarily due to the repeated processing of GPS observations within the loop. Additionally, the proposed methods show that non-diagonal VCMs based on sine and tangent models demand more memory and PT than their diagonal counterparts, owing to the extra calculations involved. Moreover, the accuracy of the positioning has significantly improved. According to Table 2 and 3, although the KF method does not have the best accuracy, it consumes less resources than PAPR methods. The trade-off between hardware usage and positioning accuracy demonstrates the effectiveness and efficiency of the proposed methods.

## 5 Conclusion

In this paper, a method was proposed to improve positioning accuracy using a single-frequency GPS receiver. In this method, the phased-adjusted pseudo-range algorithm was used to filter pseudo-range observations and reduce their noise through the use of precise phase measurements, thereby improving positioning accuracy. In addition, to determine the stochastic model, a non-diagonal VCM was used, accounting for the spatial correlations between the observations based on two different trigonometric models. Experimental results demonstrated that the proposed method outperforms other methods in terms of

stability, smoothness, and accuracy, leading to at least a 40% improvement in positioning results compared to the LS method and at least a 10% improvement compared to diagonal VCM-based methods. The hardware implementation of the proposed models using ARM technology demonstrated that the model is highly optimal, effective, and feasible. This result reflects a successful balance between model complexity and enhanced accuracy in the receiver's positioning.

## Conflict of Interest

The authors declare no conflict of interest.

## Author Contributions

**N. Rahemi:** Conceptualization, Methodology, Software, Validation, Investigation, Resources, Original draft preparation, Visualization. **K. Zarrinnegar:** Conceptualization, Software, Validation, Data curation. **M. R. Mosavi:** Supervision, Reviewing and editing, Project administration, Investigation.

## Funding

This research received no external funding.

## Informed Consent Statement

Informed consent was obtained from all subjects involved in the study.

## References

- [1] Kavathekar J.S. and Deshpande A.M., "Comparative analysis of Least Squares method and Extended Kalman filter for position estimation in GPS receiver," *Advances in Signal and Data Processing, Lecture Notes in Electrical Engineering*, Vol. 703, pp. 389-403, 2021.
- [2] Martin A., Parry M., Soundy A.W., Panckhurst B.J., Brown P., Molteno T.C. and Schumayer D., "Improving real-time position estimation using correlated noise models", *Sensors*, Vol. 20, No. 20, p. 5913, 2020.
- [3] Zhou Z., Li Y., Fu C., and Rizos C. "Least-Squares support vector machine-based Kalman filtering for GNSS navigation with dynamic model real-time correction", *IET Radar Sonar Navigation.*, Vol. 11, pp. 528-538, 2017.
- [4] Hamza V., Stopar B., Sterle O. and Pavlovčič-Prešeren P., "Observations and positioning quality of low-cost GNSS receivers: a review," *GPS Solutions*, Vol. 28, No.3, p.149, 2024.
- [5] Boguspayev N., Akhmedov D., Raskaliyev A., Kim A. and Sukhenko A., "A comprehensive review of GNSS/INS integration techniques for land and air

- vehicle applications,” *Applied Sciences*, Vol. 13, No. 8, p. 4819, 2023.
- [6] He Y., Li J. and Liu J., “Research on GNSS INS & GNSS/INS integrated navigation method for autonomous vehicles: A survey,” *IEEE Access*, 2023.
- [7] Zhang Q., Ma X., Gao Y., Huang G. and Zhao Q., “An improved carrier-smoothing code algorithm for BDS satellites with SICB,” *Remote Sensing*, Vol. 15, No. 21, pp. 5253, 2023.
- [8] Cui H., Zhang S. and Li J., “An improved phase-smoothed-code algorithm using GNSS dual-frequency carrier epoch-difference geometry-free combination observations,” *Advances in Space Research*, Vol. 71, No. 8, pp. 3433-3443, 2023.
- [9] Agarwal N. and O’Keefe K., “Use of GNSS Doppler for prediction in Kalman filtering for smartphone positioning,” *IEEE Journal of Indoor and Seamless Positioning and Navigation*, Vol. 1, pp. 151-160, 2023.
- [10] “An improved Hatch filter algorithm towards sub-meter positioning using only android raw GNSS measurements without external augmentation corrections,” *Remote Sensing*, Vol. 11, No. 14, p. 1679, 2019.
- [11] Verhagen S. and Teunissen P.J.G., *Least-squares estimation and Kalman filtering*, Springer Handbook of Global Navigation Satellite Systems, Springer: Berlin/Heidelberg, Germany, pp. 639-660, 2017.
- [12] Tang J., Lyu D. and Zeng F., “A BDGIM-based phase-smoothed pseudorange algorithm for BDS-3 high-precision time transfer,” *Applied Sciences*, Vol. 12, No. 20, p. 10246, 2022.
- [13] Banachowicz A. and Wolski A., “A comparison of the Least Squares with Kalman filter methods used in algorithms of fusion with dead reckoning navigation data,” *the International Journal on Marine Navigation and Safety of Sea Transportation*, Vol. 11, No. 4, 2017.
- [14] Rahemi N. and Mosavi M. R., “Positioning accuracy improvement in high-speed GPS receivers using sequential extended Kalman filter,” *IET Signal Processing*, Vol. 15, No. 4, pp. 251-264, 2021.
- [15] Mirmohammadian F., Asgari J., Verhagen S. and Amiri-Simkooei A., “Improvement of multi-GNSS precision and success rate using realistic stochastic model of observations,” *Remote Sensing*, Vol. 14, No. 1, pp. 60, 2021.
- [16] Luo X., Lin Y., Dai X., Bian S. and Chen D., “An improved stochastic model for the geodetic GNSS receivers under ionospheric scintillation at low latitudes,” *Space Weather*, Vol. 22, No. 2, p.e2023SW003632, 2024.
- [17] Deng J., Zhao X., Zhang A. and Ke F., “A robust method for GPS/BDS pseudorange differential positioning based on the Helmert variance component estimation,” *Journal of Sensors*, Vol. 2017, No. 1, pp. 8172342, 2017.
- [18] Zhang Q., Zhao L. and Zhou J., “A novel weighting approach for variance component estimation in GPS/BDS PPP,” *IEEE Sensors Journal*, Vol. 19, No. 10, pp. 3763-3771, 2019.
- [19] Martin A., Parry M., Soundy A.W., Panckhurst B.J., Brown P., Molteno T.C. and Schumayer D., “Improving real-time position estimation using correlated noise models”, *Sensors*, Vol. 20, No. 20, pp. 5913, 2020.
- [20] Li F., Gao J., Psimoulis P., Meng X. and Ke F., “A novel dynamical filter based on multi-epochs Least-Squares to integrate the carrier phase and pseudorange observation for GNSS measurement,” *Remote Sensing*, Vol. 12, No. 11, pp. 1762, 2020.
- [21] Kermarrec G. and Schön S., “A priori fully populated covariance matrices in Least-Squares adjustment-case study: GPS relative positioning,” *Journal of Geodesy*, Vol. 91, pp. 465-484, 2017.
- [22] Zhu M., Yu F., Xiao S., Fan S. and Wang Z., “An improved posteriori variance-covariance components estimation applied to unconventional GPS and multiple low-cost imus integration strategy”, *IEEE Access*, Vol. 7, pp. 136892-136906, 2019.
- [23] Prochniewicz D., Wezka K. and Kozuchowska J., “Empirical stochastic model of multi-GNSS measurements,” *Sensors*, Vol. 21, No. 13, pp. 4566, 2021.

### Biographies



**N. Rahemi** received her B.Sc., M.Sc., and Ph.D. degrees in Electronic Engineering from Iran University of Science and Technology (IUST), Tehran, Iran in 2011, 2013, and 2021 respectively. She is currently a faculty member (assistant professor) of the Department of Electrical Engineering of IUST. Her research interests include signal processing, artificial intelligence, and GPS applications.



**K. Zarrinegar** received his B.Sc. degree in Electrical Engineering from Ferdowsi University of Mashhad (FUM) in 2020. He received his master's degree in Integrated Circuit and Electronics Engineering at Iran University of Science and Technology (IUST). His research interests include artificial intelligence, global navigation satellite system, signal acquisition, and GNSS anti-spoofing technology.



**M. R. Mosavi** received his B.Sc., M.Sc., and Ph.D. degrees in Electronic Engineering from Iran University of Science and Technology (IUST), Tehran, Iran in 1997, 1998, and 2004, respectively. He is currently a faculty member (full professor) of the Department of Electrical Engineering of IUST. He is the author of more than 600 scientific publications in journals and international conferences in

addition to 15 academic books. His research interests include circuits and systems design. He is also editor in-chief of "Iranian Journal of Marine Technology" and editorial board member of "Iranian Journal of Electrical and Electronic Engineering" and "GPS Solutions"